Design of an ultrasound cylindrical phased-array for hyperthermia breast cancer treatment

K.W.A. van Dongen[1], J.F. Bakker[2], M.M. Paulides[2], I.M. Obdeijn[3] and G.C. van Rhoon[2]
[1] *Laboratory of Acoustical Imaging and Sound Control, Department of Imaging Science & Technology, Faculty of Applied Sciences, Delft University of Technology, The Netherlands,*
[2] *Department of Radiation Oncology, unit Hyperthermia, Erasmus MC - Daniel den Hoed Cancer Center, Rotterdam, Netherlands,*
[3] *Department of Radiology, Erasmus MC - Daniel den Hoed Cancer Center, Rotterdam, The Netherlands,*
Email: K.W.A.vanDongen@TUDelft.nl

Introduction

In the Netherlands, one out of every nine women gets breast cancer [1]. This disease has a large impact, both physically and socially Consequently, there is a need for a powerful modality to treat breast cancer. Several randomized phase III trials have demonstrated that hyperthermia (HT) cancer treatment is a powerful method to improve the clinical outcome of radiotherapy and chemotherapy [2, 3, 4, 5]. In our study we aim for breast cancer treatment by increasing the temperature to $40 - 44$°C [6].

For breast cancer, EM based hyperthermia treatment is not optimal. In the present study we explore the possibility of using ultrasound, taking advantage of its improved penetration depth and better focusing possibilities.

For ultrasound based thermal ablation therapy the operating frequencies are usually above 1 MHz, since small (< 1 mm) spot sizes are required to obtain steep temperature gradients between the tumour (up to 95°C) and the surrounding healthy tissue. Various focus scanning techniques [7, 8] are used to cover the entire target volume and to avoid large heating times. For HT however, larger volumes are heated and smaller temperature gradients are required. Therefore, larger focus sizes and lower frequencies might be suitable for reducing the need for scanning and computational resources needed for treatment planning. An additional advantage of the low frequency approach is an improved penetration advantageous for deeply located breast tumours.

Numerical Method

Approach

To investigate the feasibility of applying HT at tumors located anywhere in the intact breast, we theoretically designed an appropriate phased-array. We positioned transducers in a cylindrical configuration to obtain deep heating from the skin into the muscle layer of the chest wall. The breast is embedded in water which is used both as a coupling medium and to cool the skin. Selective tumor heating is obtained by altering the phases of the wave fields to generate adaptive interference patterns within the intact breast. The minimum required focus diameter equals approximately 5 mm. In this way we reduce the need for scanning or defocussing techniques to cover the complete tumor. Of course, larger tumors larger will still require defocussing, waveform diversity [20] or dynamic steering techniques. Consequently, our theoretical design study will therefore focus on a low-frequency (100 kHz) ultrasound phased-array for HT treatment of tumors located anywhere in the intact breast.

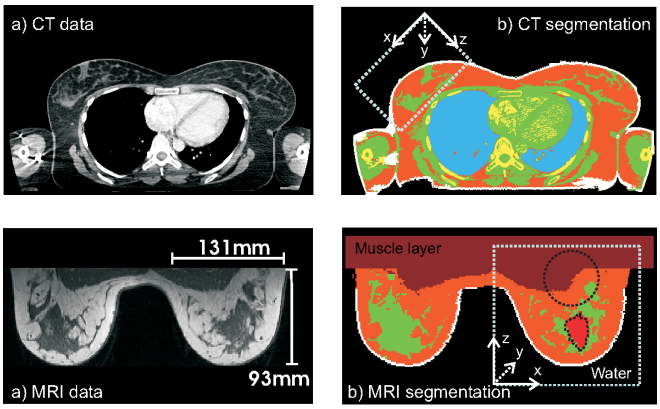

Figure 1: Synthetic breast models are constructed from CT (top-left) and MRI (bottom-left) scans. The white dotted rectangle in the segmentized scans (right) indicate the spatial domain that is used for modeling. The CT based model is used for the design, while the MRI-based model is used for characterization of SAR and temperature distributions in either the "Central tumor" ($\sim 30 \times 20 \times 38$ mm^3) or the artificial "Thorax tumor" (dotted sphere with radius of 25 mm).

Design parameters such as *(i)* number of transducers, *(ii)* ring distance and *(iii)* number of rings have been optimized to obtain a primary focus with a diameter of approximately 5 mm, while suppressing secondary foci [6]. However, during the design process we also took into account the possibilities of steering the focus within the breast, the focus size and position. In addition, the radius of the array ($r = 75$ mm) is chosen such that a single intact breast fits in the cylinder, see Figure 2. Finally, we tried to reduce the total number of transducers for economical and practical reasons without generating high amplitude secondary foci.

Tissue	ρ $\frac{\text{kg}}{\text{m}^3}$	c $\frac{\text{m}}{\text{s}}$	α_0 $\frac{\text{dB}}{\text{m}}$	k_t $\frac{\text{W}}{\text{mK}}$	c_t $\frac{\text{J}}{\text{kg K}}$	ω_b $\frac{\text{ml}}{\text{min kg}}$
Water	993	1524	0.2	0.50	4186	-
Muscle	1040	1532	120	0.50	3580	27
Fat	950	1478	35	0.24	2493	25
Skin	1200	1610	104	0.37	3496	87
Breast	1020	1485	44	0.50	2493	25
tumor	1000	1500	80	0.50	3770	330

Table 1: Acoustic and thermal medium parameters used for modeling. The absorption coefficient α_0 at $f = 1$ MHz is used to compute the absorption coefficient α according to (6), with n=1 for all tissues and n=2 for water. The thermal properties of blood are set to $\rho_b c_b = 4052910$ Jm^{-3}K^{-1}, where ρ_b and c_b are the volume density of mass and the specific heat of blood respectively. The thermal conductivity k_t and blood perfusion rate ω_b are used to compute the effective conductivity k_{eff} according to (14).

Heterogeneous breast models

The design of the apparatus is based on a synthetic model obtained from a CT scan from a breast, see Figure 1. For this model the spatial computational domain equals $175 \times 175 \times 100$ mm^3 and contains $64 \times 64 \times 32$ cubic elements.

After the design, an MRI based model has been used to demonstrate the potential of the theoretical design by modeling SAR and temperature distributions for breast tumors. In this case, the dimensions of the model are $160 \times 160 \times 160$ mm^3 containing $128 \times 128 \times 128$ elements. In addition to the segmented "Central tumor", a deeply (4-9 cm from the skin) located "Thorax tumor" is mimicked by an artificial sphere. The medium parameters for all tissues are listed in table 1.

Pressure wave field

The acoustic pressure field is modeled using the scalar wave equation in the temporal Laplace domain with Laplace parameter $\hat{s}$. Frequency domain results are obtained by taking the limit $\hat{s} \rightarrow -j\omega$, with $j^2 = -1$ and ω the temporal angular frequency. The symbol "$\hat{}$" on top of a parameter is used to show it's frequency dependency. The incident pressure field $\hat{p}^{\text{inc}}$ is the field that would be present if the object ("obj") shows no acoustical contrast with respect to the background ("bg"). The total pressure field $\hat{p}^{\text{tot}}$ at position $\mathbf{r}$ in the three-dimensional spatial domain $\mathbb{D}$ can be written as a superposition of the incident, $\hat{p}^{\text{inc}}$, and the scattered pressure field, $\hat{p}^{\text{scat}}$, according to [9]

$$\hat{p}^{\text{tot}}(\mathbf{r}) = \hat{p}^{\text{inc}}(\mathbf{r}) + \hat{p}^{\text{scat}}(\mathbf{r}), \tag{1}$$

with

$$\hat{p}^{\text{inc}}(\mathbf{r}) = \hat{s}\rho_{\text{bg}} \int_{\mathbf{r}' \in \mathbb{D}^{\text{src}}} \hat{G}(\mathbf{r} - \mathbf{r}')\, \hat{q}(\mathbf{r}')\, \mathrm{d}V, \tag{2}$$

$$\hat{p}^{\text{sct}}(\mathbf{r}) = \int_{\mathbf{r}' \in \mathbb{D}^{\text{s}}} \hat{G}(\mathbf{r} - \mathbf{r}') \left[\hat{k}_{\text{bg}}^2 - \hat{k}_{\text{obj}}^2(\mathbf{r}')\right] \hat{p}^{\text{tot}}(\mathbf{r}')\, \mathrm{d}V \tag{3}$$

where ρ_{bg} is the volume density of mass of the background medium, $\hat{q}$ is a volume density of injection rate source in the domain $\mathbb{D}^{\text{src}}$ representing the transducer, and $\hat{k}_{\text{bg}}$ and $\hat{k}_{\text{obj}}$ are the complex wave numbers of the background medium in $\mathbb{D}$ and the object medium in the sub-domain $\mathbb{D}^{\text{s}}$ that contains the contrast. The Green's function $\hat{G}$ equals

$$\hat{G}(\mathbf{r} - \mathbf{r}') = \frac{e^{-j\hat{k}_{\text{bg}}|\mathbf{r}-\mathbf{r}'|}}{4\pi|\mathbf{r} - \mathbf{r}'|} \tag{4}$$

and is singular for $\mathbf{r} = \mathbf{r}'$. Therefore, its weak form [12] is used in the actual computation scheme. Note that equation (1) represents an integral equation. This can be solved using a conjugate gradient inversion scheme [10, 11].

Specific Absorption Rate

The total pressure fields are used to compute the local mass Specific Absorption Rate (SAR). The local absorption of energy is accounted for in (3) via the complex wave number $\hat{k}$, which is defined as

$$\hat{k} = \hat{k}_0 - j\hat{\alpha}, \tag{5}$$

where $\hat{k}_0 = \omega/c$ is the real valued wave number of the lossless background medium with c the speed of sound of the background medium. The amplitude attenuation coefficient $\hat{\alpha}$ for tissues appears to increase with frequency according to [13]

$$\hat{\alpha}(\mathbf{r}) = \alpha_0(\mathbf{r})\, f^n, \tag{6}$$

where α_0 is the absorption coefficient at $f = 1$ MHz and n is found experimentally. The acoustic heat production volume density rate $\hat{Q}$ can be expressed as

$$\hat{Q}(\mathbf{r}) = -\nabla \cdot \hat{\mathbf{I}}(\mathbf{r}) = -\nabla \cdot \frac{1}{2}\mathrm{Re}\left\{\hat{p}^{\text{tot}}(\mathbf{r})\, \hat{\mathbf{v}}^{\text{tot}*}(\mathbf{r})\right\}, \tag{7}$$

where $\hat{\mathbf{I}}$ is the energy flow, $-\nabla \cdot \hat{\mathbf{I}}$ denotes the rate at which acoustic energy is transported to an element of the medium per unit volume and $\hat{\mathbf{v}}^{\text{tot}*}$ is the complex conjugate of the total particle velocity. For any continuous steady-state single-frequency field the particle velocity can be eliminated [14] resulting in

$$\text{SAR}(\mathbf{r}) = \frac{\hat{Q}(\mathbf{r})}{\rho(\mathbf{r})} = \hat{\alpha}(\mathbf{r})\, \frac{|\hat{p}^{\text{tot}}(\mathbf{r})|^2}{\rho(\mathbf{r})^2\, c(\mathbf{r})}. \tag{8}$$

Input power normalization

The total input power of the phased-array is normalized to 1 W by altering the volume density of injection rate $\hat{q}_i$ of each transducer according to

$$\hat{q}_i^{norm} = \hat{q}_i \frac{1}{\sum_{i=1}^{N} W_i}, \tag{9}$$

where W_i is the radiated power for transducer i, which is found by integrating the far-field ($\hat{k}_{0,\text{bg}}|\mathbf{r} - \mathbf{r}'| >> 1$) monopole intensity [15] over the surface of a sphere centered at the source $\hat{q}_i$, resulting in

$$W_i = \frac{{\hat{q}_i}^2 \hat{k}_{\text{bg}}^2 \rho_{\text{bg}} c_{\text{bg}}}{4\pi}. \tag{10}$$

Focusing with the TCP method

Focusing is obtained by altering the phases of the RF signals to correct for the various path lengths from each transducer toward the Target Center Position (TCP), $\mathbf{r}_{tcp}$, where maximum interference is required. Assuming an homogeneous speed of sound, $\hat{q}_i$ is modified into

$$\hat{q}_i^{tcp}(\mathbf{r}_i) = \hat{q}_i e^{j\varphi_i}, \tag{11}$$

where the phase φ_i of transducer i at $\mathbf{r}_i$ is given by

$$\varphi_i = |\mathbf{r}_i - \mathbf{r}_{tcp}| \frac{\omega}{c_{\mathrm{bg}}}. \tag{12}$$

Thermal model

Temperature patterns are computed by using a thermal model that describes the heat transfer in tissues. The model is based on Pennes Bio Heat Equation (PBHE) [16] and is formulated as,

$$\rho_t c_t \frac{\partial T_t}{\partial t} = \nabla \cdot (k_t \nabla T_t) + \rho_t Q_m + \rho_t \mathrm{SAR} - \rho_b c_b \rho_t \omega_b (T_t - T_b), \tag{13}$$

where ρ_t is the volume density of mass, c_t is the specific heat, k_t is the thermal conductivity and T_t is the temperature of tissue "t"; c_b, ρ_b and T_b are the specific heat, volume density of mass and temperature (37°C) of the blood "b"; ω_b is the blood perfusion rate and Q_m is the metabolic heat generation rate (neglected in this work). For simplicity the spatial dependency ($\mathbf{r}$) and time of observation (t) are left out (13).

The effective conductivity model used in this work is defined as [17]

$$k_{eff}(\mathbf{r}) = k_t(\mathbf{r})\{1 + C\omega_b(\mathbf{r})\}, \tag{14}$$

where the constant $C = 0.01$ is obtained experimentally [18]. The breast is embedded in water which is kept constant at 30°C and maximum heat transfer is assumed, so a Dirichlet boundary condition ($T = T_{\mathrm{boundary}}$) is applied at the interface. The spatial domain $\mathbb{D}$ is thermally insulated, i.e. no heat passes this interface. The SAR is scaled such that the maximum steady state temperature is 44°C. The PBHE, the effective conductivity model and the thermal boundary conditions are discretized and solved with a Finite Difference Time Domain (FDTD) technique [19], which is implemented in SEMCAD X (Schmid & Partner Engineering AG, Switzerland).

Results

The design parameters number of transducers per ring, ring distance and number of rings have been investigated and resulted in the configuration shown in Figure 2. For this phased-array configuration, SAR and temperature distributions are obtained for both the MRI-based "Central tumor" and the artificial "Thorax tumor".

Figures 3a and 3b show that, for both tumor locations, the maximum SAR is found in the tumor center, however

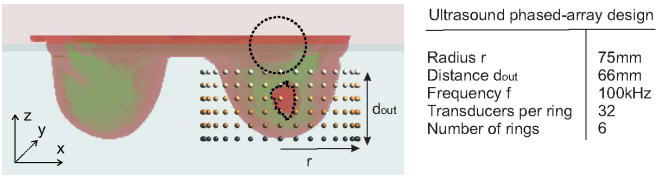

Figure 2: Ultrasound cylindrical phased-array design result. The mesh of little spheres indicates the position of the monopole transducers and the black dotted lines indicate the contours of the tumor and target region.

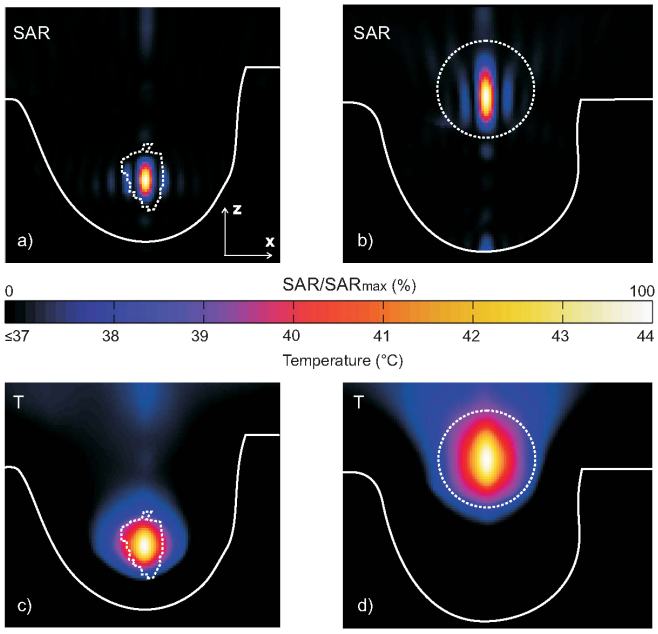

Figure 3: SAR (a,b) and temperature (c,d) distributions in planes through the tumor center for the "Central tumor" (a,c) and the "Thorax tumor" (b,d). The white solid and dotted lines indicate the breast and tumor contours respectively.

the tumors are not covered homogeneously. Although not shown here, all SAR foci are located at equal positions as in the $|\hat{p}^{\mathrm{inc}}|^2$ interference patterns, indicating a minimum influence of the heterogeneous acoustic tissue properties. Figures 3c and 3d demonstrate that, for both tumor locations, maximum 44°C is obtained in the tumor center without any hot spots, however the tumors are not heated homogeneously. The temperature maximum is located at the same position as the SAR maximum and no hot or cold spots are observed elsewhere in the breast, indicating a minimum influence of the heterogeneous thermal tissue properties.

Discussion and conclusion

Using a "low" frequency results in a good penetration depth and reduced scattering effect by small-sized heterogeneities in the breast anatomy ($\lambda \approx 15$ mm at f = 100 kHz). An additional practical advantage is that the reduced frequency reduces the required computational resources for adequate treatment planning.

Furthermore the TCP method, which assumes a homogeneous wave velocity profile, predicted the $\mathrm{SAR}_{\mathrm{max}}$ location within an accuracy of 1 mm. Hence, for this

study, it would have been sufficient to use homogeneous breast models and to use the Born approximation, which simplifies the total pressure integral equation and consequently also further reduces the total computation time.

The results, see Figure 3, show that the dimensions of the volumes enclosed by the 41°C iso-temperature are 19×19×21 mm^3. Therefore, either electrical or mechanical steering techniques are still required to heat larger volumes. In this work we used the TCP method to create the smallest possible focus, however defocussing, waveform diversity [20] or dynamic steering techniques might be used to enlarge the treatment volumes.

Simulations predict that an ultrasound cylindrical phased-array, consisting of six rings with 32 transducers per ring, a radius of 75 mm and 66 mm distance between the first and sixth transducer ring, operating at a frequency of 100 kHz, can be used to obtain 44°C in the center of either centrally or deeply located breast tumors. The dimensions of the 50% iso-SAR_{max} volume are 6×6×14 mm^3. The dimensions of the volumes enclosed by the 41°C iso-temperature are 19×19×21 mm^3 and 21×21×32 mm^3 for central and deep locations respectively. Consequently, with this applicator it will become feasible to effectively heat tumors located anywhere in the intact breast. In addition, it is demonstrated that acoustic and thermal heterogeneities do not disturb the SAR and temperature patterns within the breast.

References

[1] KWF Kanker Bestrijding. URL: `http://www.kwfkankerbestrijding.nl/`

[2] Comparison of radiotherapy alone with radiotherapy plus hyperthermia in locally advanced pelvic tumors: a prospective, randomised, multicentre trial. Lancet **355** (2000) 1119–1125

[3] Multicentric study comparing intravesical chemotherapy alone and with local microwave hyperthermia for prophylaxis of recurrence of superficial transitional cell carcinoma. J Clin Oncol **21** (2003) 4270-4276

[4] Prospective thermal dosimetry: the key to hyperthermia's future. Int J Hyperthermia **22** (2006), 247-253

[5] Radiotherapy with or without hyperthermia in the treatment of superficial localized breast cancer: results from five randomized controlled trials. International Collaborative Hyperthermia Group. Int J Radiat. Oncol. Biol. Phys. **35** (1996) 731-744

[6] An ultrasound cylindrical phased-array for deep heating in the breast: theoretical design using heterogeneous models. submitted to Phys Med Biol

[7] Ultrasound surgery: comparison of strategies using phased array systems. IEEE Transactions on Ultrasonics, Ferroelectrics and Frequency Control. **43**(6) (1996) 1085–1098

[8] Scanning path optimization for ultrasound surgery. Phys Med Biol **50** (2005) 3473-3490

[9] Handbook of Radiation and Scattering of Waves: Acoustic Waves in Fluids, Elastic Waves in Solids, Electromagnetic Waves. Academic Press, London, 1995

[10] A reduced forward operator for acoustic scattering problems. IEE Conference Publications **2005**(CP511) (2005) 294-299

[11] A full vectorial contrast source inversion scheme for three-dimensional acoustic imaging of both compressibility and density profiles. J Acoust Soc Am **121**(3) (2007) 1538-1549

[12] The Three-Dimensional Weak Form of the Conjugate Gradient FFT Method for solving Scattering Problems. IEEE Transactions on Microwave Theory and Techniques **40**(9) (1992)

[13] Methods of External Hyperthermic Heating, Clinical Thermology. subseries Thermotherapy, Springer-Verlag, 1990

[14] Heat generation by ultrasound in a relaxing medium. J Acoust Soc Am (1981) **70**(2)

[15] Engineering Noise Control, Theory and Practice. Spon Press, 2003

[16] Analysis of tissue and arterial blood temperature in the resting human forearm. J Appl Physiol **1** (1948) 93-122

[17] A new simplified bioheat equation for the effect of blood flow on local average tissue temperature. J Biomech Eng **107**(2) (1985) 131–139

[18] Experimental verification of bioheat transfer theories: Measurement of temperature profiles around large artificial vessels in perfused tissue. Phys Med Biol **35** (1990) 905–923

[19] Novel conformal technique to reduce staircasing artifacts at material boundaries for FDTD modeling of the bioheat equation. Phys Med Biol **52** (2007) 4371-4381

[20] Waveform diversity based ultrasound system for hyperthermia treatment of breast cancer. IEEE Trans Biomed Eng **55**(2) (2008), 822-826